CONTINUOUS STRUCTURAL MONITORING USING STATISTICAL PROCESS CONTROL

Hoon Sohn[†], Michael L. Fugate[‡], and Charles R. Farrar[†]

† Engineering Sciences & Applications Division, Engineering Analysis Group, M/S C926
‡ CIC Division, Computer Research & Applications Group, M/S B265
Los Alamos National Laboratory, Los Alamos, NM 87545

1. ABSTRACT

A damage detection problem is cast in the context of a statistical pattern recognition paradigm. In particular, this paper focuses on applying statistical process control methods referred to as "control charts" to vibration-based damage detection. First, an auto-regressive (AR) model is fitted to the measured time histories from an undamaged structure. Residual errors, which quantify the difference between the prediction from the AR model and the actual measured time history at each time interval, are used as the damage-sensitive features. Next, the average and variability of the selected features are monitored by the X-bar and S control charts. A statistically significant number of error terms outside the control limits indicate a system transit from a healthy state to a damage state. For demonstration, this statistical process control is applied to vibration test data acquired from a concrete bridge column as the column is progressively damaged

2. INTRODUCTION

The potential economic impact and life-safety implications of early damage detection in aerospace, civil and mechanical engineering systems has motivated a significant amount of research in structural health monitoring. Many local damage detection methods have been developed and are routinely applied to a variety of structures [4]. Because of its potential for global system monitoring, damage detection as determined from changes in the vibration characteristics of a system has been a popular research topic for the last thirty years. Doebling et al. (1998) present a recent thorough review of these vibration-based damage identification methods [5]. While the references cited in this review propose many different methods for extracting damage-sensitive features from vibration response measurements, few of the cited references take a statistical approach to quantifying the observed changes in these features. However, because all vibration-based damage detection processes rely on experimental data with inherent uncertainties, statistical analysis procedures are necessary if one is to state in a quantifiable manner that changes in the vibration response of a structure are indicative of damage as opposed to operational and environmental variability. This paper will first pose the general problem of the vibration-based damage detection process in the context of a problem in statistical pattern recognition. A damage detection study of a seismically retrofitted, reinforced concrete bridge pier is then described in the context of this paradigm. This discussion emphasizes the application of a statistical analysis procedure referred to as statistical process control (SPC) to the vibration-base damage detection problem. Although SPC is a well-established condition monitoring procedure for rotating machinery [11], the authors are not aware of applications of this technology to the vibration-based damage detection problem that includes civil infrastructures.
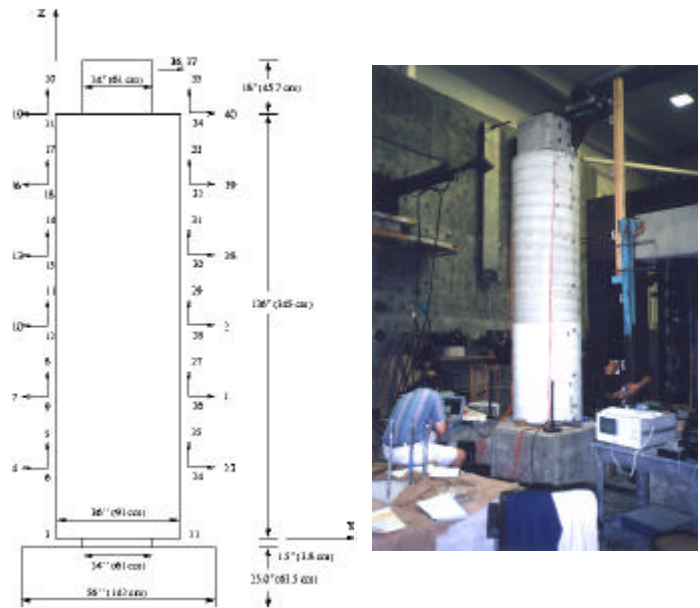
3. TEST SETUP

Figure 1: Dimensions and photo of an actual test structure.

Faculty, students and staff at the University of California, Irvine (UCI) performed quasi-static, cyclic tests to failure on seismically retrofitted, reinforced-concrete bridge columns. Vibration tests were performed on the columns at intermittent stages during the static load cycle testing when various amounts of damage had been accumulated in the columns. The associated data obtained from one of the columns are used to investigate the applicability of statistical pattern

recognition techniques to vibration-based damage detection problem.

3.1 Structure Description

The configuration and dimension of the test column the dimensions are shown in
Figure 1. The test structure was a 137.5 in (349 cm) long, 24 in (61 cm) diameter concrete bridge column that was subsequently retrofitted to a 36 in (91 cm) diameter column. The column was retrofitted by placing forms around the existing column and placing additional concrete within the form. A 24 in^2 concrete block, which had been cast integrally with the column, extended 18 in (46 cm) above the top of the circular portion of the column. This block was used to attach the hydraulic actuator to the column for quasi-static cyclic testing and to attach the electro-magnetic shaker used for the vibration tests. The column was bolted to the testing floor with 25 in (63.5 cm) thick in the UCI laboratory during both the static cyclic tests and vibration tests.

3.2 Test Procedure

A hydraulic actuator was used to apply lateral loads to the top of the column in a quasi-static, cyclic manner. The loads were first applied in a force-controlled manner to produce lateral deformations at the top of the column corresponding to $0.25 \Delta y_T$, $0.5 \Delta y_T$, $0.75 \Delta y_T$ and Δy_T. Here, Δy_T is the lateral deformation at the top of the column corresponding to the theoretical first yield of the longitudinal reinforcement. The structure was cycled three times at each of these load levels. Next, a lateral deformation corresponding to the actual first yield Δy was estimated based on the observed response. Loads were then applied in a displacement-controlled manner, again in sets of three cycles, at displacements corresponding to $1.5 \Delta y$, $2.0 \Delta y$, $2.5 \Delta y$, etc. until the ultimate capacity of the column was reached.

Vibration tests were conducted on the column in its undamaged state, and after cycling loading at the subsequent displacement levels, Δy, $1.5 \Delta y$, $2.5 \Delta y$, $4.0 \Delta y$, and $7.0 \Delta y$. In this study, these vibration tests are referred to as damage level 0 thought 5, respectively. The excitation for the vibration tests was provided by an APS electro-magnetic shaker mounted off-axis at the top of the structure. The shaker rested on a steel plate attached to the top square block of the concrete column. Horizontal loading was transferred from the shaker to the structure through a friction connection between the shaker and the steel support plate. The shaker was controlled in an open-loop manner while attempting to generate 0 - 400 Hz uniform random signal. The RMS voltage level of this signal remained constant during all vibration tests. However, feedback from the column and the dynamics of the mounting plate produced an input signal that was not uniform over the specified frequency range.

4. STATISTICAL PATTERN RECOGNITION PARADIGM

In the context of statistical pattern recognition the process of vibration-based damage detection can be broken down into four parts: (1) Operational Evaluation, (2) Data Acquisition and Cleansing, (3) Feature Extraction and Data Compression, and (4) Statistical Model Development.

4.1 Operational Evaluation

Operational evaluation begins to set the limitations on what will be monitored and how to perform the monitoring as well as tailoring the monitoring to unique aspects of the system and unique features of the damage that is to be detected.

Because the structure being tested was a laboratory specimen, operational evaluation was not conducted in a manner that would typically be applied to an *in situ* structure. The vibration tests were not the primary purpose of this investigation. Therefore, compromises had to be made regarding the manner in which the vibration tests were conducted. The primary compromise was associated with the mounting of the shaker where it would have been preferable to suspend the shaker from soft supports and apply the input at a point location using a stinger. These compromises are analogous to operational constraints that may occur with *in situ* structures. Environmental variability was not considered an issue because the tests were conducted in a laboratory setting. The available dynamic measurement hardware and software placed the only constraints on the data acquisition process.

4.2 Data Acquisition and Cleansing

The *data acquisition* portion of the structural health monitoring process involves selecting the types of sensors to be used, the location where the sensors should be placed, the number of sensors to be used, and the data acquisition/storage/transmittal hardware. *Data cleansing* is the process of selectively choosing data to accept for, or reject from, the feature selection process. Filtering is one of the most common methods for data cleansing.

Forty accelerometers were mounted on the structure as shown in
Figure 1. These locations were selected based on the initial desire to measure the global bending, axial and torsional modes of the column. Note that locations 2, 39 and 40 had a nominal sensitivity of 10mV/g and were not sensitive enough for the measurements being made. As part of the data cleansing process, data from these channels were not used in subsequent portions of the damage detection process. Locations 33, 34, 35, 36, and 37 were accelerometers with a nominal sensitivity of 100mV/g. All other channels had accelerometers with a nominal sensitivity of 1V/g. An accelerometer on the sliding mass of the shaker provided a measure of the input force applied to the column. Analog signal from the accelerometers was sampled and digitized with a Hewlett-Packard (HP) 3566A dynamic data acquisition system. Data acquisition parameters were specified such that unwindowed 8-second time-histories with discretized 8192 points were acquired.

Anti-aliasing filters were applied to further cleanse the data. An analog anti-aliasing filter with a cut off frequency of 12.8 kHz was used along with a digital anti-aliasing filter with a cut off frequency of 512 Hz. Data decimation was also used to cleanse the data. Although the data are sampled at 25.6 kHz, the decimation process yields an effective sampling rate of

1.024 kHz. Finally, an AC coupling filter that attenuates signal below 2 Hz was applied to remove DC offsets from the signal.

4.3 Feature Extraction

The area of the structural damage detection process that receives the most attention in the technical literature is *feature extract*. Feature extraction is the process of the identifying damage-sensitive properties derived from the measured vibration response that allows one to distinguish between the undamaged and damaged structures.

One of the main assumptions in the use of control charts is the independence of the extracted features. Conventional control charts indicate too frequent false-positive warnings if the selected features exhibit high levels of correlation over time. Therefore, the correlation in the raw time history data needs to be removed prior to the application of control charts. As a feature extraction process of this study, an AR model is fitted to the time history data in order to remove the correlation. An AR model with *p* auto-regressive terms can be written:

$$x(t) = a + \sum_{j=1}^{p} f_j \ x(t-j) + z(t) \qquad (1)$$

This is referred to as an AR(*p*) model. $x(t)$ is the observed time history at time t, f_j is an auto-regression coefficient, and $z(t)$ is an unobservable random error with zero mean and constant variance. The mean of $x(t)$ for all t is m. The f_j's are estimated by fitting the AR model obtained from the undamaged structure, and $a \equiv \left(1 - \sum f_j\right) m$. In this study, the AR coefficients are estimated by using the Yule-Walker method [3].
Denoting $\hat{x}(t)$ as the predicted time history from the fitted AR model at time *t*, the residual error $e(t) = x(t) - \hat{x}(t)$ is defined as the damage sensitive feature to be used in this study. Note that $e(t)$ is an estimate of $z(t)$ in Equation (1). When new data become available, the response at the current time point is predicted using *p* past time points and the previously fitted AR(*p*) model. Then, the residual errors are computed for $t = p+1, \ p+2, \dots$. The assumption in using this residual error feature is that the AR model derived from data measured on the undamaged structure will show greater residual errors when it is used to predict the response measured on the damaged structure. Consequently, changes in the mean and/or variance of the residuals should be observed. The following X-bar and S control charts provide a statistical framework to detect these changes.

4.4 Statistical Model Development

The portion of the structural health monitoring process that has received the least attention in the technical literature is the development of statistical models to enhance the damage detection process. *Statistical model development* is concerned with the implementation of the algorithms that analyze the distributions of the extracted features in an effort to determine the damage state of the structure.

Statistical process control (SPC) is a collection of tools useful in process monitoring, and improvement. The control chart is the most commonly used one and very suitable for automated continuous monitoring. A control chart provides a framework for continuously monitoring future measurements and for identifying new data that are inconsistent with past data. In this study, the two most commonly used control charts, the *X-bar* and *S control charts*, are employed for damage diagnosis. Several variations of the X-bar and S charts can be found in Reference [9]. When the system of interest experiences abnormal conditions, the mean, the variance of the extracted features, or both are expected to change. The X-bar control chart provides a framework for monitoring the changes of the selected feature mean and the S chart measures the variability of the features over time.

4.4.1 X-bar Control Chart

The X-bar control chart provides a framework for monitoring the changes of the selected feature means and for identifying samples that are inconsistent with the past data. To monitor the mean variation of the features, the features are first arranged in *m* subgroups of size *n*:

$$
\begin{matrix}
t_{11} & t_{12} & \cdots & t_{1n} \\
t_{21} & t_{22} & \cdots & t_{2n} \\
\vdots & \vdots & & \vdots \\
\vdots & \vdots & & \vdots \\
t_{m1} & t_{m1} & \cdots & t_{mn}
\end{matrix}
\qquad (2)
$$

where t_{ij} is the extracted feature from previous section, *i.e.*, the residual $e(t)$ in this study. *m* is the number of samples (or subgroups), and *n* is the size of individual sample. The sample size *n* is often taken to be 4 or 5. If *n* is chosen too large, a drift that may be present in individual sample mean may be obscured, or averaged-out. An additional motivation for the rational subgrouping, as opposed to individual observations, is that the distribution of the samples means can be reasonably approximated by a normal distribution as a result of the central limit theorem. Next, the sample mean $\overline{X}_i$ and standard deviation S_i of the features are computed for each sample ($i = 1, \cdots, m$):

$$\overline{X}_i = mean\left(t_i^j\right) \text{ and } S_i = std(t_i^j) \qquad (3)$$

Here the mean and standard deviation are with respect to *n* observations in each sample.

Finally, a control chart is constructed by drawing a centerline (CL) at the mean of the sample means and two additional horizontal lines corresponding to the upper and lower control limits (UCL & LCL) versus sample numbers (or with respect to time). The centerline and two control limits are defined as follows:

$$CL = mean(\overline{X}_i), \text{ and UCL, LCL} = CL \pm Z_{a/2} \frac{S}{\sqrt{n}} \qquad (4)$$

where the calculation of mean is with respect to all samples ($i = 1, \cdots, m$). $Z_{a/2}$ is the percentage point of the normal distribution with zero mean and unit variance such that $P[z \geq Z_{a/2}] = a/2$. The variance S^2 is estimated by averaging the variance S_i of all samples:

$$S^2 = mean(S_i^2) \qquad (5)$$

Note that, regardless of the distribution of t, $\overline{X}_i$ can be approximated by a normal distribution as a result of the central limit theorem. Therefore, the control limits in Equation (4) correspond to a $100(1-a)\%$ confidence interval. In many practical situations, the distribution of features may not be exactly normal. However, it has been shown that the control limits based on the normality assumption can be often successfully used unless the population is extremely non-normal [9].

If the system experienced damage, this would likely be indicated by an unusual number of sample means outside the control limits: a charted value outside the control limits is referred to as an *outlier* in this paper. Finally, the monitoring of damage occurrence is performed by plotting $\overline{X}_i$ values obtained from the new data set along with the previously constructed control limits. In general, observing a significant number of samples outside the control limits does not necessarily indicate that the structure is damaged. However, since there was no significant variation of environment or operational conditions during the column test of this study, the deterioration of the structure was assumed to be the main cause of the abnormal changes of the system.

4.4.2 Construction of S Control Chart

Similar to the X-bar control chart, the variability of individual subgroup S_i can be monitored by the S control chart. To construct the S control chart, CL, UCL and LCL are defined as follows:

$$CL = mean(S_i), \quad UCL = S\sqrt{\frac{c_{1-a/2, n-1}^2}{n-1}} \text{ and}$$
$$LCL = S\sqrt{\frac{c_{a/2, n-1}^2}{n-1}} \qquad (6)$$

where $c_{1-a/2, n-1}^2$ and $c_{a/2, n-1}^2$ denote the upper and lower percentage points of the chi-square distribution with $n-1$ degrees of freedom.

Note that the rational subgroup plays an important role in the use of X-bar and S control charts. The sample size should be selected to maximize the process mean changes between samples (for X-bar chart) and to measure only the instantaneous process variability within a sample (for S control chart). In other word, the X-bar control chart monitors between-sample variability and the S control chart measures within-sample variability only.

5. EXPERIMENTAL RESULTS

The applicability of the X-bar and S control charts to damage diagnosis problems is demonstrated using the vibration test data obtained from the test column shown in Figure 1. In this paper, the diagnosis results using only the time series obtained from measurement point one of Figure 1 is presented. Although the results obtained from the other accelerometers are not presented here, similar results are observed for most of measurement points.

As mentioned earlier, the time series obtained at individual damage level are 8-second long and comprise 8192 time points. First, the issue of the AR order selection is addressed and AR(5) is chosen for this study. The selected AR(5) model is fitted to the time series obtained from the intact structure so as to estimate the AR coefficients. The differences between the measured time series and the prediction from the AR(5) are computed for damage level 0 producing 8187 ($= 8192 - 5$) residual terms. Four consecutive residuals are then grouped together resulting in 2046 samples each of size 4. The last three residual terms are simply disregarded. Note that the extracted feature t (the residual error in this study) is standardized prior to the construction of the control charts. The sample mean is subtracted from the feature and the feature is normalized by the standard deviation. Therefore, CL for all figures in this paper corresponds to zero. Next, the control limits corresponding to a 99% confidence interval are constructed by setting $a = 0.01$ in Equations (4) and (6). After the construction of the control limits, damage diagnoses using the X-bar and S control charts are performed for the subsequent damage levels 1 through 5. Finally, the robustness of the control charts against false-positive warning of damage is tested using the two separate sets of time histories obtained from the intact state of the column.

5.1 Order Selection of the AR Model

Prior to the feature selection, an appropriate order of the AR model needs to be determined. There exist several model selection techniques such as Akaike Information Criterion (AIC) and Bayesian Information Criterion (BIC) to validate the goodness of fit for the selected AR model [2]. However, because the construction of control charts using correlated data produces an underestimated the sample variance and increase the possibility of a false positive alarm, the model order selection in this study is mainly based on the analysis of the autocorrelation functions.

The autocorrelation analysis shows that the correlation of the original time series over time is still significant for time lags around 70-80. To remove the correlation an AR(5) is fitted to the original time series data. AR(5) successfully removes most of correlation: Correlation of the residual error $e(t)$ is significantly reduced compared to that of the original time history $x(t)$. The AR(5) model has reduce all the correlation to less than 0.20, and most correlation to less than 0.10. In particular, the correlation is nearly 0 for time lag 1-3. Recall that the subgroups are formed by placing 4 consecutive residuals together. This grouping means that the maximum time lag within a sample is 3, and the residuals within each

sample are essentially uncorrelated. Because the residuals within each subgroup are nearly uncorrelated, the sample variance within each sample is for practical purposes an unbiased estimate of the population variance.

A number of higher order AR models were fitted to the data without significantly improving the correlation reduction of AR(5). For example, an AR(19) model, which was the best fit model based on AIC, eliminated most of the autocorrelation through lag 30, but there still existed statistically significant correlation beyond lag 30. Furthermore, the performance of the control charts using AR(19) was not significantly better than that of AR(5). Auto-regressive moving-average (ARMA) models were also tried but the results were the same as with fitting higher order AR models. At this time no compelling reason was found to fit a model more complicated than AR(5).

5.2 X-Bar Control Chart Analysis

The X-bar control chart monitors the sample means from each subgroup. Figure 2 shows the damage diagnosis results using the previously estimated AR(5) model. CL, UCL, and LCL denote the centerline, upper and lower control limits estimated from the time series of the undamaged structure, respectively.

The outliers, which are samples outside the control limits, are marked by "+" sign in all figures. Note that the extracted feature t (the residuals in this case) is standardized prior to the construction of the X-bar control chart. The sample mean is subtracted from the feature and the feature is normalized by the standard deviation. Therefore, CL for all figures in this paper corresponds to zero, and UCL and LCL are accordingly normalized.

Because of the choice of $a = 0.01$, approximately 20 samples (= 1 % of total 2046 samples) are expected to be outside the control limits even when the system is in control. Therefore, 13 outliers in Figure 2 (a) do not indicate any system anomaly for damage level 0. However, a statistically significant number of outliers are observed for the rest of damage levels 1 though 5.

5.3 S Control Chart Analysis

Similar to the X-bar chart analysis, a monitoring of the sample variance is performed using S control chart. Again the control limits corresponding to the 99% confidence interval are computed using the undamaged time series data. Then, the process monitoring is conducted for all damage levels.
Figure 3 shows the damage diagnosis results using the previously estimated AR(5) model. 16 outliers are observed for damage level 0 implying the appropriate construction of the control limits. A statistically significant number of outliers are again observed for all damage levels. In particular, the shifting of the sample standard deviation above UCL indicates broadening of the extracted feature distribution at different damage levels.

5.4 False Positive Alarm Testing

While it is desirable to have features sensitive to damage, the monitoring system also needs to be robust against false-positive indication of damage (false-positive indication of damage means that the monitoring system indicates damage although no damage is present). To investigate the robustness of the proposed control charts against false-positive warning of damage, two separate tests are designed. In the first test, the time histories obtained from the undamaged state of the test structure are divided into two parts. The first half of the time series is employed to construct the control limits, and the false-positive testing is carried out using the second half of the time series.
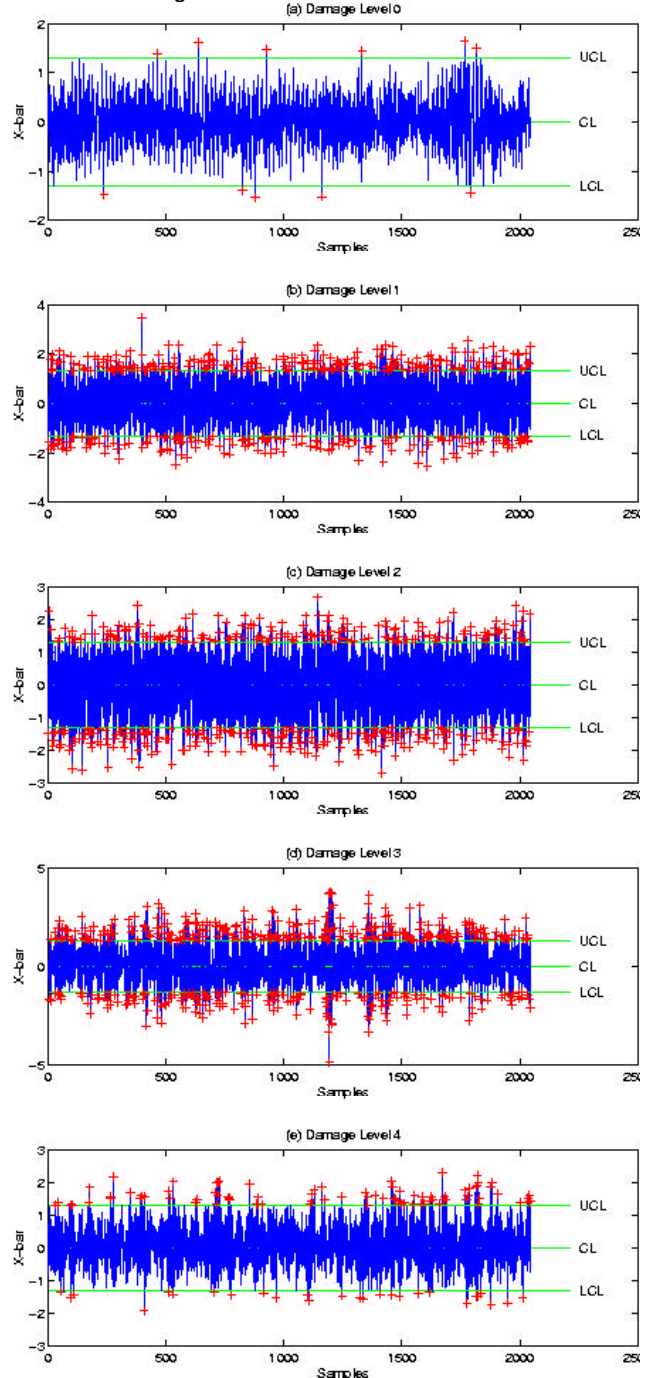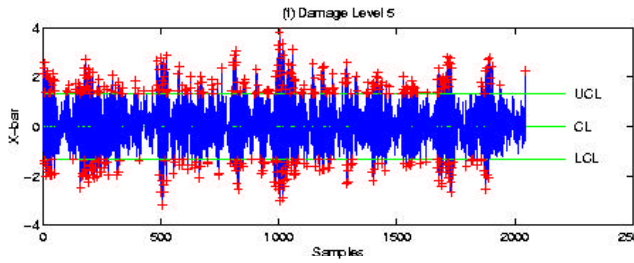
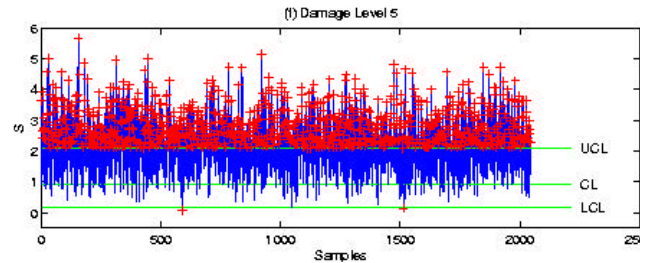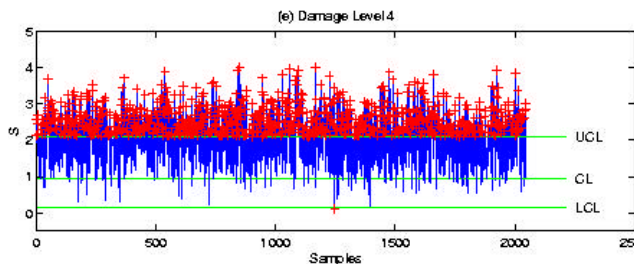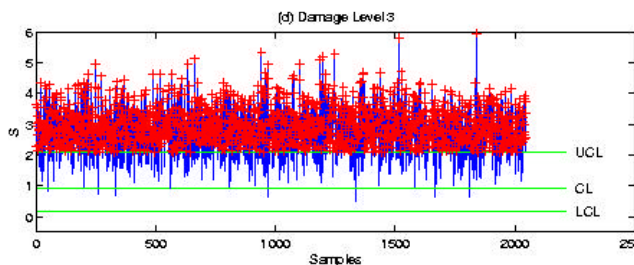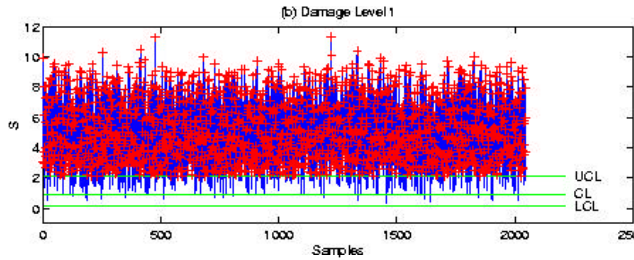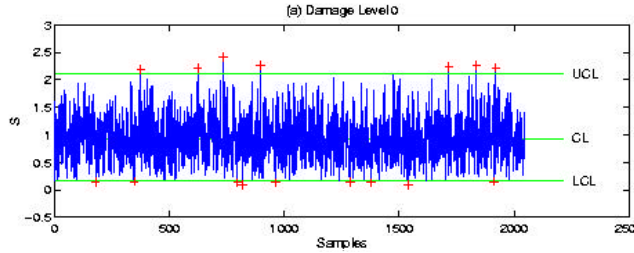Figure 2: X-bar control chart of the residual errors
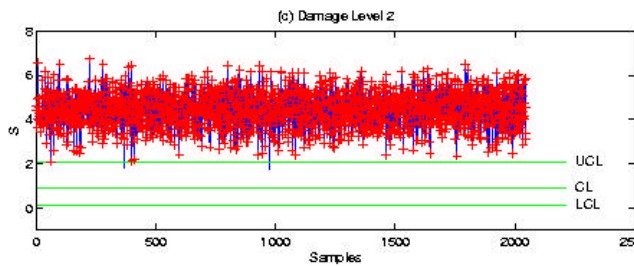
Figure 3: S control chart of the residual errors

Note that the original time series are 8-second long with 8192 time points, and each half of the time series is 4-second long and has 4096 points. That is, an AR(5) model is fitted to the first half of the time series estimating the AR coefficients. The residuals are then computed from the second half of the time series resulting in 1023 samples of size 4.

Figure 4 (a) shows the construction of the X-bar chart using the first half of the time series. In addition, the fluctuation of the features extracted from the first half time series is also plotted together. The false-positive testing using the second half of the time series is presented in Figure 4 (b).

For the second test, the control limits are established using the whole 8-second time histories from the undamaged state of the column, and the false-positive test is conducted using an independent 2-second time series measured from a separate vibration test of the undamaged column. The results of damage diagnoses are presented in Figure 4 (c). For all the cases, the number of outliers are less than 10 (1 % of total sample number 1023). Similar results are also observed for the S control chart. The two sets of tests presented here have demonstrated that damage diagnosis using the control charts appears to be robust against false-positive indication of damage for the data studied.
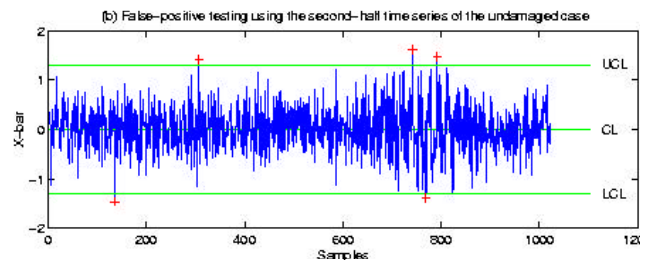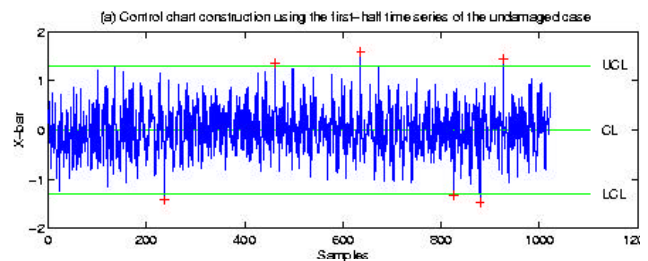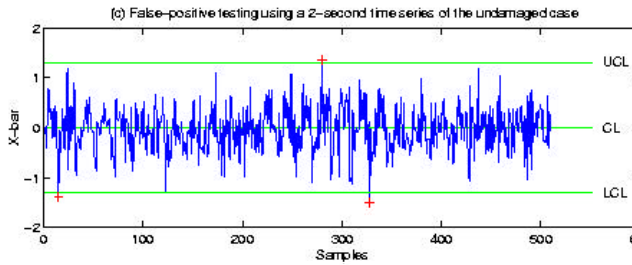
Figure 4: False-positive testing using X-bar control chart

6. SUMMARY AND CONCLUSIONS

This paper has presented vibration-based damage detection problems in the context of statistical pattern recognition. In particular, statistical process control using control charts is applied to the vibration test data obtained from the bridge column. In this study, two most commonly used control charts, X-bar and S control charts, are employed for damage diagnosis. The X-bar control chart monitors the process mean of a system, and the S chart measures the variability of the process over time. After the construction of the control limits, damage diagnoses using the X-bar and S control charts are performed for the subsequent damage levels 1 through 5. The robustness of the proposed control charts against false-positive warning of damage (indication of damage when none is present) is also demonstrated using two separate tests. In this paper, damage diagnosis is conducted by identifying outliers charted outside the control limits. This outlier detection is primary useful to detect moderate-to-large process shifts. Small shifts in a system can be also detected by analyzing trends in the control chart. For example, if there were a repeated pattern of 5 consecutive samples above the mean, this non-random trend could be an indicative of damage. A variety of other measures are also available to detect small shifts [9].

In general, the observation of a large number of outliers does not necessary indicate that the structure is damaged but only that system has varied to cause statistically significant changes in its vibration signatures. This variability can be caused by a variety of environmental and operational conditions that the system of interest is subject to. Because the influence of operational and environmental factors on the dynamic characteristics of the test structure is minimal for the presented laboratory test, the feature selection and the subsequent statistical process control have been carried out assuming that system deterioration is mainly responsible for the changes of vibration characteristics. However, operational and environmental conditions such as wind, humidity, intensity and frequency of traffic loading should be taken into account for applications of full-scale civil infrastructures. This fact necessitates a continuous monitoring of the *in-site* structure to let the statistical model learn the underlying patterns of the environmental and operational variability. The presented control chart analysis can be easily adopted to monitor system integrity when a stream of measurement data is continuously available. A joint research effort with Kinemetrics Corporation is currently underway to develop a multivariate, continuous control chart to incorporate such additional factors to the statistical patter recognition paradigm presented in this study.

REFERENCES

[1] Bishop, C. M., *Neural Networks for Pattern Recognition*, Oxford University Press, Oxford, UK, 1995.

[2] Box, G. E., Jenkins, G. M., and Reinsel, G. C., *Time Series Analysis: Forecasting and Control*, Prentice-Hall, Inc., 1994.

[3] Brockwell, P. J. and Davis, R. A., *Time Series: Theory and Methods*, Springer, New York, 1991.

[4] Doherty, J. E., "Nondestructive Evaluation," Chapter 12 in *Handbook on Experimental Mechanics*, A. S. Kobayashi Edt., Society for Experimental Mechanics, Inc., 1987

[5] Doebling, S. W., Farrar, C. R., Prime , M. B., and Shevitz, D. W., "A Review of Damage Identification Methods that Examine Changes in Dynamic Properties," *Shock and Vibration Digest* **30** (2), pp. 91-105, 1998.

[6] Farrar, C. R., and Jauregui, D. V., "A Comparative Study of Damage Identification Algorithms Applied to a Bridge: Part I: Experimental" *J. of Smart Materials and Structure,* **7,** 1998.

[7] Hunter, N. F., "Bilinear System Characterization from Nonlinear Time Series Analysis," *17th IMAC*, Orlando, FL, 1999.

[8] Martin, H. R., "Statistical Moment Analysis as a Means of Surface Damage Detection," *7th IMAC*, Las Vegas, NV, 1989.

[9] Montgomery, D. C., *Introduction to Statistical Quality Control*, John Wiley & Sons, Inc., New York, 1996.

[10] Prime, M. B. and Shevitz, D. W., "Linear and Nonlinear Methods for Detecting Cracks in Beams," *14th IMAC*, Dearborn, MI, 1996.

[11] Wowk, V., *Machinery Vibration Measurement and Analysis*, McGraw-Hill, Inc. New York, 1991.